Article

Not peer-reviewed version

Synergistic Antitumor Effects of 177Lu-Octreotide Combined with an ALK Inhibitor in a High-Risk Neuroblastoma Xenograft Model

Arman Romiani , Daniella Pettersson , Nishte Rassol , Klara Simonsson , Hana Bakr , Dan Emil Lind , Aniko Kovacs , Johan Spetz , Ruth H Palmer , Bengt Hallberg , Khalil Helou , Eva Forssell-Aronsson *

Posted Date: 5 March 2024

doi: 10.20944/preprints202403.0251.v1

Keywords: Neurobastoma; Radionuclide therapy; Apoptosis; Somatostatin analog; Radiosensitization; Combination therapy

Article

Synergistic Antitumor Effects of ^{177}Lu-Octreotide Combined with an ALK Inhibitor in a High-Risk Neuroblastoma Xenograft Model

Arman Romiani [1,2], Daniella Pettersson [1,2], Nishte Rassol [1,2], Klara Simonsson [1,2], Hana Bakr [1,2,3], Dan Emil Lind [2,4], Aniko Kovacs [2,5], Johan Spetz [1,2], Ruth H Palmer [2,4], Bengt Hallberg [2,4], Khalil Helou [2,6] and Eva Forssell-Aronsson [1,2,3,*]

1 Department of Medical Radiation Sciences, Institute of Clinical Sciences, Sahlgrenska Academy, University of Gothenburg, Gothenburg, Sweden
2 Sahlgrenska Center for Cancer Research, Sahlgrenska Academy, University of Gothenburg, Gothenburg, Sweden
3 Medical Physics and Biomedical Engineering, Sahlgrenska University Hospital, Gothenburg, Sweden
4 Department of Medical Biochemistry and Cell Biology, Institute of Biomedicine, Sahlgrenska Academy, University of Gothenburg, Gothenburg, Sweden
5 Department of Pathology, Institute of Clinical Sciences, Sahlgrenska Academy, University of Gothenburg, Gothenburg, Sweden
6 Department of Oncology, Institute of Clinical Sciences, Sahlgrenska Academy, University of Gothenburg, Gothenburg, Sweden
* Correspondence: eva.forssell_aronsson@radfys.gu.se

Simple Summary: Patients with high-risk neuroblastoma often have poor prognoses and limited treatment options. Radiopharmaceutical treatment with ^{177}Lu-labeled peptides that target somatostatin receptors on the neuroblastoma tumor cells have been proposed for therapy, as have inhibitors of the receptor tyrosine kinase anaplastic lymphoma kinase (ALK), which is frequently mutated in these patients. The aim of this study was to evaluate the effects of combining these two treatment modalities on overall tumor growth and induction of cell death in human neuroblastoma tumors grown in mice. Results show that the combination had greater effects on the tumors than the sum of the effects from the separate treatments, and also induced cell death in the tumor cells. Taking advantage of the tumor-seeking properties of both treatments, better treatment results of disseminated high-risk neuroblastoma may be achieved.

Abstract: Neuroblastoma (NB) is a childhood cancer with heterogeneous characteristics, posing challenges to effective treatment. NBs express somatostatin receptors that facilitates the use of somatostatin analogs (SSTAs) as tumor-seeking agents for diagnosis and therapy. High-risk (HR) NBs often have gain-of-function mutations in the receptor tyrosine kinase anaplastic lymphoma kinase (ALK). Despite intensive multimodal treatment, survival rates remain below 40% for children with HR-NB. The aim of this work was to investigate the combined effect of the SSTA ^{177}Lu-octreotide with the ALK inhibitor lorlatinib. Mice bearing human HR-NB CLB-BAR tumors were treated with lorlatinib, ^{177}Lu-octreotide, combination of these pharmaceuticals or saline (control). Tumor volume was monitored and tumor samples were evaluated for cleaved caspase-3 and expression of 84 human genes involved in apoptosis. Combination treatment with ^{177}Lu-octreotide and lorlatinib demonstrated synergistic antitumor effects. Increased number of cleaved caspase 3-positive cells was observed in tumors from mice treated with ^{177}Lu-octreotide alone and in combination with lorlatinib. Modulation of *Bcl-2* family gene expression was observed only in the presence of both ^{177}Lu-octreotide and lorlatinib, with *BID* downregulated and *HRK* upregulated on days 2 and 7, respectively. The data suggests that ALK signaling pathway inhibition may contribute to radiosensitization in radionuclide therapy with ^{177}Lu-octreotide.

Keywords: neuroblastoma; radionuclide therapy; apoptosis; somatostatin analog; ALK-inhibitor; radiosensitization

 doi:10.20944/preprints202403.0251.v1

1. Introduction

Anaplastic lymphoma kinase (ALK) is a receptor tyrosine kinase (RTK), a member of the insulin RTK family, which is expressed in the developing central and peripheral nervous system [1]. ALK dimerization, in response to ALKAL ligand binding, activates signaling pathways involved in various cellular processes, such as proliferation, transcription, growth, and survival [1]. Mutated, rearranged, or amplified *ALK* in a wide range of tumors acts as an oncogene. ALK overexpression has been identified in several tumor types, including ovarian cancer, breast cancer, and neuroblastoma (NB). Among newly diagnosed high-risk (HR) NB patients, *ALK* mutations or gene amplification occur in approximately 14% [2–4]. Previous studies have illustrated the cooperativity of ALK and MYCN, the major oncoprotein of HR-NB [5–7]. Despite intensive multimodal treatment, and significant improvements, survival rates remain less than 40% for children with HR-NB [8].

Lorlatinib is a potent ALK inhibitor (ALKi) that binds to the ATP binding site of the ALK kinase domain, preventing ALK downstream signaling [9]. Lorlatinib was FDA-approved in 2018 for treatment of ALK-positive metastatic non-small-cell lung cancer and has demonstrated robust antitumor effects in comparison with other ALKis [10–12]. Classified as a third-generation ALKi, lorlatinib demonstrates activity against several drug-resistant *ALK* mutations [11]. Phase I trials have been reported in patients with ALK-positive NB, both as monotherapy and in combination, with manageable toxicity profiles and antitumor effects [13,14]. Despite this, studies suggest that treatment with lorlatinib can still lead to drug resistance [15–18], strengthening the need to understand the underlying mechanisms of drug resistance and highlighting the need to identify combination therapy options.

^{177}Lu-[DOTA0,Tyr^{3}]octreotide (^{177}Lu-octreotide) is a radiopharmaceutical that binds to somatostatin receptors (SSTRs) [19–21]. Octreotide is a synthetic somatostatin analog (SSTA) with high affinity for SSTR2 [22]. ^{177}Lu is a beta-emitting radionuclide with a half-life of 6.7 days. The range of the emitted electrons ($E_{\beta max}$ = 497 keV) is <2 mm in tissue, which is well suited for disseminated tumors [23–25]. The closely related radiopharmaceutical, ^{177}Lu-octreotate, is FDA- and EMA-approved for treatment of gastroenteropancreatic neuroendocrine tumors. Previous preclinical and clinical studies have demonstrated selective uptake and therapeutic potential from the use of radiolabeled SSTAs for SSTR-positive HR-NB, however, the modest therapy effect in some of the studies highlights the need for optimization of these treatments [26–29]. An ongoing phase II study with ^{177}Lu-octreotate is now being conducted where an individualized treatment regimen is reviewed for children with relapsed HR-NB (Neuroblastoma-LuDO-N) [30].

With the treatment-resistance properties of HR-NB, combination treatments with radionuclide therapy and ALKi could be beneficial. The aim of this work was to examine the effects of combination treatment with lorlatinib and ^{177}Lu-octreotide on growth and expression of apoptosis-related genes in the tumors of NB-bearing mice.

2. Materials and Methods

2.1. Tumor Cell Line and Animal Model

The study was performed with CLB-BAR (ALK gain of function, *Δexon4–11* truncated ALK; MYCN amplification) NB cells obtained from The Center Leon Berard, France under MTA. [31]. CLB-BAR cells were cultured as previously described [26]. A mixture of matrigel (Corning, 354248, VWR, USA) and 1.5×10^{6} CLB-BAR cells were injected s.c. into the flank of 5-6 weeks old female BALB/c nude mice (Janvier Labs, France). All animal experiments were approved by the Swedish Ethical Committee on Animal Experiments in Gothenburg (ethical reference number 2779-20) and carried out following guidelines from Animal Research: Reporting of In Vivo Experiments (ARRIVE).

 doi:10.20944/preprints202403.0251.v1

2.2. Pharmaceuticals

Lorlatinib (Selleckchem, Houston, Texas, United States) was formulated in 2% DMSO, 30% PEG300, and double-distilled water. The solution was prepared for oral gavage with 10 mg/kg for each mouse.

^{177}Lu-octreotide was prepared according to the manufacturer's requirements (ITG Isotope Technologies Garching GmbH, München, Germany). Instant thin layer chromatography (ITLC-SG, chromatography paper 50/PK, Varian, USA), with 0.1 M of sodium citrate as the mobile phase, was implemented to determine the radiochemical purity, which was above 97%. The specific activity of ^{177}Lu-octreotide was 66 MBq/μg, yielding approximately 0.47 μg peptide for 30 MBq ^{177}Lu-octreotide. ^{177}Lu activity in each syringe was measured with an ionization chamber (CRC-15R, Capintec, Inc., New Jersey, USA) before and after injection, to determine the actual administered activity to each mouse.

2.3. Treatment Regimens

Tumor bearing mice were divided into four groups (n=10 mice/group). Mean tumor volume was 480 mm^3 (SEM=30 mm^3) at treatment start. Groups were treated with either 1) lorlatinib via daily oral gavage (from day 0 to day 14), 2) with a single i.v. injection with 30 MBq ^{177}Lu-octreotide on day 1, or 3) a combination of both treatments. The fourth group acted as a control and received an i.v. injection with saline on day 1.

Mouse weight and tumor volume was measured four times per week. Tumor volume was calculated based on measurements using digital calipers of the three perpendicular axes (a, b, and c) of the tumor: $V = \frac{4\pi abc}{3}$.

Three mice from each group were sacrificed on day 2 and three on day 7, and the remaining four mice in each group on day 14. At sacrifice, the animals were under anesthesia with pentobarbitalnatrium (vet. 60 mg/ml, Apotek Produktion & Laboratorier AB, Sweden) injected i.p. before cardiac puncture. Tumor samples from each time point (days 2, 7, and 14) were collected and divided into two parts, one placed in vials with formalin for immunohistochemical (IHC) analysis and the other freshly frozen in liquid nitrogen and stored at -80℃ for real-time reverse transcription polymerase chain reaction (qPCR) analysis.

2.4. Immunohistochemical Analysis

After fixation in formalin, tumor samples were embedded in paraffin, sectioned (thickness 4 μm), deparaffinized, rehydrated, and processed with the DAKO EnVision FLEX antigen retrieval EDTA buffer pH 9 using the DAKO PT Link (PT Link, Denmark) [26]. IHC staining was performed with anti-cleaved caspase-3 (CC3) (1:100, #9661, Cell Signaling Technology, MA, USA). Digital images were captured with a 40× magnification using a Panoramic Scanner P250 from 3DHISTECH at Histocenter AB (Mölndal, Sweden), with software, CaseViewer, Slide Converter.

IHC-scoring was implemented using the semi-quantitative Histoscore method:

$$Histoscore = \big((1 \times \%\, weak) + (2 \times \%\, moderate) + (3 \times \%\, strong)\big),$$

calculated based on the assessment of the intensity of the staining (graded: 0, negative; 1, weak; 2, moderate; or 3, strong) and the percentage of positive cells.

2.5. Gene Expression Analyses

RNA was extracted from tumor samples using a phenol-chloroform method (RNeasy Lipid Tissue Mini Kit, QIAGEN, Valencia, USA). RNA purity, integrity, and concentration were assessed with a Nanodrop 1000 Spectrometer (Thermo Scientific) (260/280 > 1.8), Agilent 2100 Bioanalyzer (Agilent Technologies) (RIN >8), and a Qubit 3.0 Fluorometer (Thermo Fisher Scientific), respectively. cDNA was subsequently generated via reverse transcription (RT^2 First Strand Kit, QIAGEN, 4 Valencia, USA) and mixed with RT^2 SYBR Green Mastermix (QIAGEN, Valencia, USA) before aliquoting in a 96-well RT^2 Profiler PCR Array for human apoptosis (PAHS-012Z, QIAGEN, Valencia,

Preprints.org (www.preprints.org) | NOT PEER-REVIEWED | Posted: 5 March 2024 doi:10.20944/preprints202403.0251.v1

USA). Totally, 84 key genes involved in the apoptosis pathway were included, where 52, 24, and 8 were classified as pro-apoptotic, apoptosis-related, and anti-apoptotic genes, respectively, classified according to the manufacturer and the Gene Ontology (GO) database.

The cycle threshold (Ct) values obtained were converted to ΔCt values based on the gene of interest versus the geometric mean of the housekeeping genes (*ACTB*, *B2M*, *GAPDH*, *HPRT1*, and *RPLP0*). Thereafter, the mean relative ΔΔCt was calculated for each treatment in relation to the mean ΔCt of the vehicle control group. By implementing the $2^{-\Delta\Delta Ct}$ method, treated *vs*. control, we obtained a fold change (FC) value for each gene [32]. Genes were defined as differentially expressed if $|FC| > 1.5$.

2.6. Statistical Analyses

All calculations and statistical analyses were made with GraphPad Prism 9.4.1.681 (GraphPad Software, CA, USA) and Excel 2013 for Windows (Microsoft Corporation, WA, USA). The relative tumor volume (RTV) was determined individually for each mouse and time-point, and mean value and the standard error of the mean (SEM) were calculated for each group. One-way ANOVA was used for estimating the statistical differences regarding tumor volume between all groups throughout the treatment period. Student's t-test was applied for comparison between groups. $P < 0.05$ was considered statistically significant different.

A theoretical additive effect of both monotherapies was calculated based on The Bliss independence model [33,34]. Firstly, the fractional response, F, of each monotherapy was estimated in relation to vehicle control

$$F_{monotherapy} = 1 - \frac{RTV_{monotherapy}}{RTV_{control}}$$

Subsequently, the theoretical additive effect was estimated

$$F_{additive} = F_{Lorlatinib} + F_{^{177}Lu-octreotide} - F_{Lorlatinib} \times F_{^{177}Lu-octreotide}$$

The theoretical value was calculated for days 4 to 14 and illustrated as a dashed line in Figure 1C.

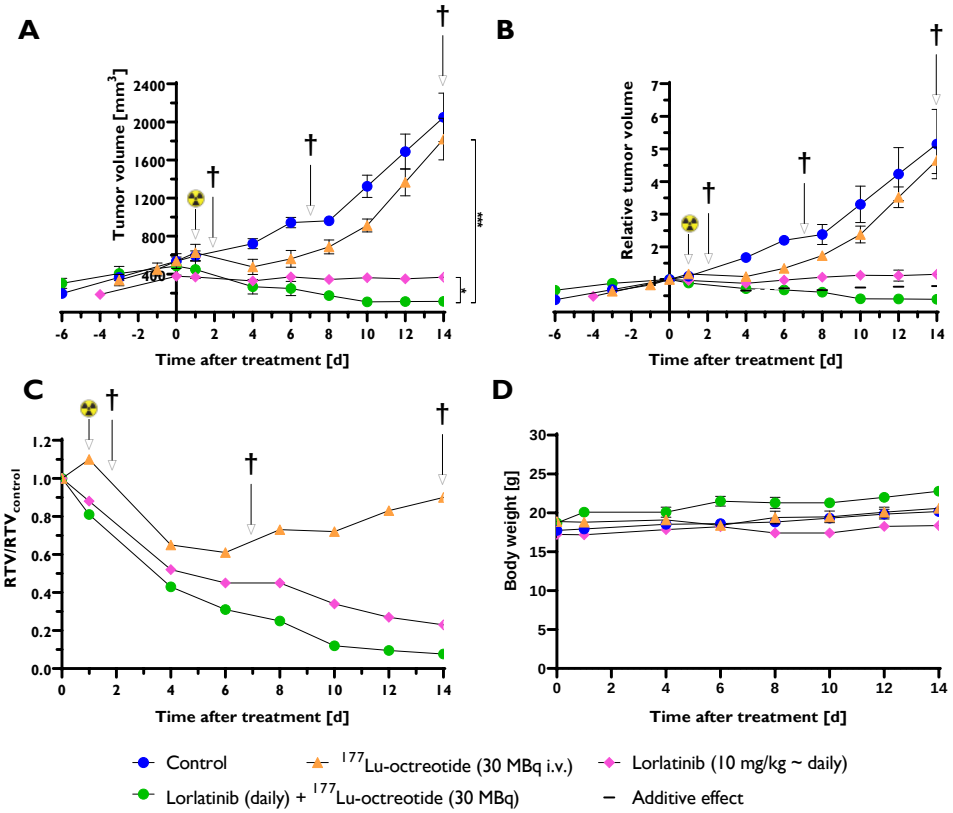

 doi:10.20944/preprints202403.0251.v1

Figure 1. Effect of treatment with either lorlatinib (pink), ^{177}Lu-octreotide (orange) or both in combination (green) in mice bearing human CLB-BAR NB xenografts on tumor volume (**A-C**) and body weight (**D**). Mice were treated with lorlatinib (daily gavage, 10 mg/kg), and/or ^{177}Lu-octreotide (30 MBq i.v. on day 1) or i.v. injected with saline on day 1 (control) (n=10 mice/group on day 0). The effect of each monotherapy and the combination therapy is shown as mean tumor volume (mm^3) (**A**) and relative tumor volume (RTV) (**B**). A theoretical additive effect was calculated using the Bliss independence model (Bliss C. 1939) and presented as a dashed line in (**B**). (**C**) The RTV-ratio ($RTV/RTV_{control}$) for all treated groups is shown. Three mice from each group were sacrificed (†) on day 2 and day 7, respectively, and the remaining four mice in each group were sacrificed on day 14. Whole body weight of each group is presented in (**D**). Error bars represent SEM, not always visible in (**D**) because of their low values, * indicates $p<0.05$ and *** $p<0.0001$.

For mRNA expression analyses, Student's t-tests were applied to compare ΔCt-values of deregulated genes post-treatment with vehicle control. $p < 0.05$ was considered statistically significant.

For immunohistochemical analyses, a Jarque-Bera test for normality showed that the Histoscores for CC3 staining did not have a normal distribution (P-value < 0.001), possibly due to the low number of samples. Because of this, the non-parametric Kruskal-Wallis test with Dunn's Multiple Comparison Test was used to compare differences between groups.

3. Results

3.1. Combination Therapy Gave the Largest Tumor Volume Reduction

BALB/c nude mice with sc CLB-BAR NB xenografts were treated with either lorlatinib, ^{177}Lu-octreotide or both in combination over 14 days. Combined therapy with both lorlatinib and ^{177}Lu-octreotide yielded the greatest antitumor effect with a RTV of 0.39 at day 14 (Figures 1A-B). Corresponding RTV value at day 14 for lorlatinib monotherapy was 1.2. ^{177}Lu-octreotide as monotherapy (i.v. injection at day 1) demonstrated an initial decrease in RTV compared to control, with the lowest RTV of 1.1 on day 4, after which RTV increased to 4.6 on day 14 and displayed similar tumor growth as control group from day 8 to 14. RTV decreased between days 1 and 4 by 7.1%, 9.8%, and 19% for ^{177}Lu-octreotide monotherapy, lorlatinib monotherapy and combination therapy, respectively. The RTV in controls increased monotonic reaching 5.2 on day 14. Combination therapy showed a more prominent antitumor effect than the theoretical value of the additive effect of both monotherapies combined from day 6 (Figure 1B).

To further illustrate the differences between each treatment versus control, we calculated the RTV ratio ($RTV_{therapy}/RTV_{control}$ (RTV-ratio) over the 14 day treatment (Figure 1C). ^{177}Lu-octreotide monotherapy resulted in a decrease in RTV-ratio on day 4 that continued until day 6 and then gradually increased. In contrast, the RTV-ratios of the lorlatinib and combination treatment groups decreased throughout the treatment period and reached 0.23 and 0.08 on day 14, respectively. One-way ANOVA demonstrated a significant difference between all groups from day 4 to 14, with $p<0.001$ at all studied time-points. No significant weight loss was observed in any group (Figure 1D).

3.2. Changes in the Expression of Genes Involved in Apoptosis

To better understand the effect of treatment on CLB-BAR xenograft growth we harvested tumors at days 2, 7 and 14 of treatment and performed qPCR analyses for 84 selected genes, including pro-apoptotic genes (Figure 2) and anti-apoptotic and apoptosis-related genes (Figure 3). Lorlatinib treatment resulted in mRNA expression changes in 5 of the 79 detected transcripts from the 84 gene panel ($|FC| > 1.5$). In response to lorlatinib, all significantly regulated genes were down-regulated, two genes (*TNFRSF9* and *BIRC3*) were found after 7 days and four genes (*CASP8, CD40, BIRC3* and *BNIP3L*) were found 14 days post-treatment. Three pro-apoptotic genes were down-regulated in comparison with control: *CASP8*, *CD40*, and *TNFRSF9* (Figure 2). *BIRC3*, categorized as anti-

 doi:10.20944/preprints202403.0251.v1

apoptotic, was down-regulated after 7 and 14 days (Figure 3). *BNIP3L*, categorized as apoptosis-related, was down-regulated after 14 days (Figure 3).

Lorlatinib			^{177}Lu-octreotide			Lorlatinib + ^{177}Lu-octreotide			
2d	7d	14d	2d	7d	14d	2d	7d	14d	
FC (-/+)	FC (-/+)	FC (-/+)	FC (-/+)	FC (-/+)	FC (-/+)	FC (-/+)	FC (-/+)	FC (-/+)	Gene
-0.13	0.08	-0.13	-0.17	0.02	-0.02	-0.32	0.01	-0.03	ABL1
-0.29	-0.56	-0.12	-0.28	-0.03	0.63	-0.50	-0.23	0.10	AIFM1
-0.26	-0.14	-0.43	0.12	0.10	0.16	0.91	0.19	0.04	APAF1
0.12	0.18	0.11	0.23	0.95	0.50	1.08	0.17	0.84	BAD
0.19	0.21	0.15	0.24	0.12	-0.11	-0.22	-0.11	0.40	BAK1
0.06	-0.15	-0.23	0.87	0.82	0.37	0.88	0.21	0.29	BAX
					-1.62				BCL2A1
0.42	-0.20	-0.56	0.49	0.57	-0.22	1.81	0.78	-0.31	BCL2L11
0.11	0.26	0.60	-0.28	-0.24	-0.10	-1.62	-0.63	-0.14	BID
0.41	0.82	0.07	0.49	0.90	0.38	1.32	0.49	0.76	BIK
0.67	0.11	0.17	0.27	0.25	0.45	1.20	0.97	0.98	BRAF
			-1.82		-0.26			1.13	CASP1
-0.16	-1.26	-0.95	0.14	0.72	-0.99	-0.17	0.83	-0.27	CASP10
									CASP14
0.01	0.15	0.01	0.07	0.25	0.09	-0.40	-0.62	0.28	CASP2
-0.39	0.34	0.67	-0.11	0.39	0.71	-0.95	-0.12	0.75	CASP3
-0.87	-0.96	-0.05	-0.20	-0.04	0.08	-0.48	-0.89	-0.01	CASP4
							2.22		CASP5
-0.21	-0.17	-1.15	0.16	0.80	0.38	-0.21	-0.08	-0.74	CASP6
0.02	-0.36	-0.39	0.20	0.08	0.43	0.07	-0.73	-0.71	CASP7
-0.43	-0.86	-1.62	-0.14	0.33	-0.63	-0.54	-0.46	-1.78	CASP8
0.04	-0.25	-0.05	-0.18	0.71	-0.10	1.83	1.96	-0.17	CASP9
-0.80	-1.47	-2.34	0.11	1.16	-0.31	0.72	0.73	-1.22	CD40
0.04	0.15	0.28	0.03	0.29	0.05	-0.34	-0.21	0.63	CIDEB
0.32	0.35	-0.52	0.54	-0.24	-0.53	-0.23	-0.70	-0.84	CRADD
0.22	0.28	0.16	0.44	0.91	-0.26	0.15	-0.09	0.57	CYCS
0.99	0.74	0.56	0.78	1.15	0.85	0.41	0.35	1.06	DAPK1
0.04	0.01	0.43	-0.01	-0.10	0.14	-0.33	-0.35	0.47	DFFA
0.00	0.12	-0.08	-0.31	0.08	-0.20	-0.05	-0.20	0.24	DIABLO
0.03	0.56	0.43	-0.47	0.28	0.25	-0.04	-0.26	0.08	FADD
0.06	-0.64	-0.50	0.96	0.80	-0.11	1.83	1.01	0.72	FAS
-0.43	0.25	0.84	0.88	0.31	-1.60	1.79	1.37	0.29	FASLG
-0.63	-0.26	-1.00	0.03	0.09	-0.32	2.04	-0.18	-0.40	GADD45A
0.19	-0.04	-0.66	-0.13	0.95	1.13	3.35	3.02	0.80	HRK
	1.48	-0.88	-1.24	1.41	-1.07		3.04	-0.03	LTA
		-0.56		0.91	-0.61		4.78		LTBR
-0.04	-0.19	-0.28	-0.05	0.20	0.08	-0.45	-0.33	0.32	NOD1
0.16	1.00	0.88	0.15	1.27	0.70	0.77	1.11	1.46	PYCARD
-0.26	-0.30	-0.37	-0.14	0.08	0.09	0.11	-0.14	-0.08	RIPK2
0.09	-0.87	-1.29	1.91	1.36	-0.20	2.75	1.15	-0.61	TNFRSF10A
-0.46	-0.82	-1.23	0.68	0.41	-0.03	1.23	-0.46	-0.33	TNFRSF10B
									TNFRSF11B
-0.01	0.47	-0.29	0.21	1.12	0.32	1.18	0.34	0.75	TNFRSF1A
0.56	1.03	-1.06	1.12	2.43	-1.11	2.10	1.46	0.20	TNFRSF1B
-0.09	-0.05	0.12	-0.35	0.50	0.41	-1.01	-0.09	0.40	TNFRSF21
	-1.52	0.26		0.27	0.65				TNFRSF9
0.11	0.03	-0.47	0.71	0.52	-1.19	1.42	1.22	-0.34	TNFSF10
0.40	0.71	0.14	0.67	1.70	-1.64				TNFSF8
-0.09	-0.19	-0.32	-0.32	-0.04	-0.03	-0.19	-0.21	-0.21	TP53BP2
									TRADD
-0.12	0.41	0.50	0.12	0.56	0.52	-0.11	-0.26	0.73	TRAF2
0.27	-0.16	0.23	0.44	0.49	0.62	0.57	-0.27	0.99	TRAF3

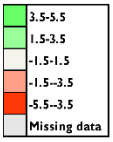

Pro-apoptotic genes

Figure 2. mRNA expression of 52 pro-apoptotic genes in tumor tissue (CLB-BAR) from mice treated with lorlatinib and/or ^{177}Lu-octreotide, expressed as fold change (FC) relative to controls. Tumors were analysed from mice were sacrificed on day 2 (n=3), day 7 (n=3) or day 14 (n=4). Red and green colors represent down- and up-regulation, respectively, with $|FC| > 1.5$. Missing data are represented by gray color.

 doi:10.20944/preprints202403.0251.v1

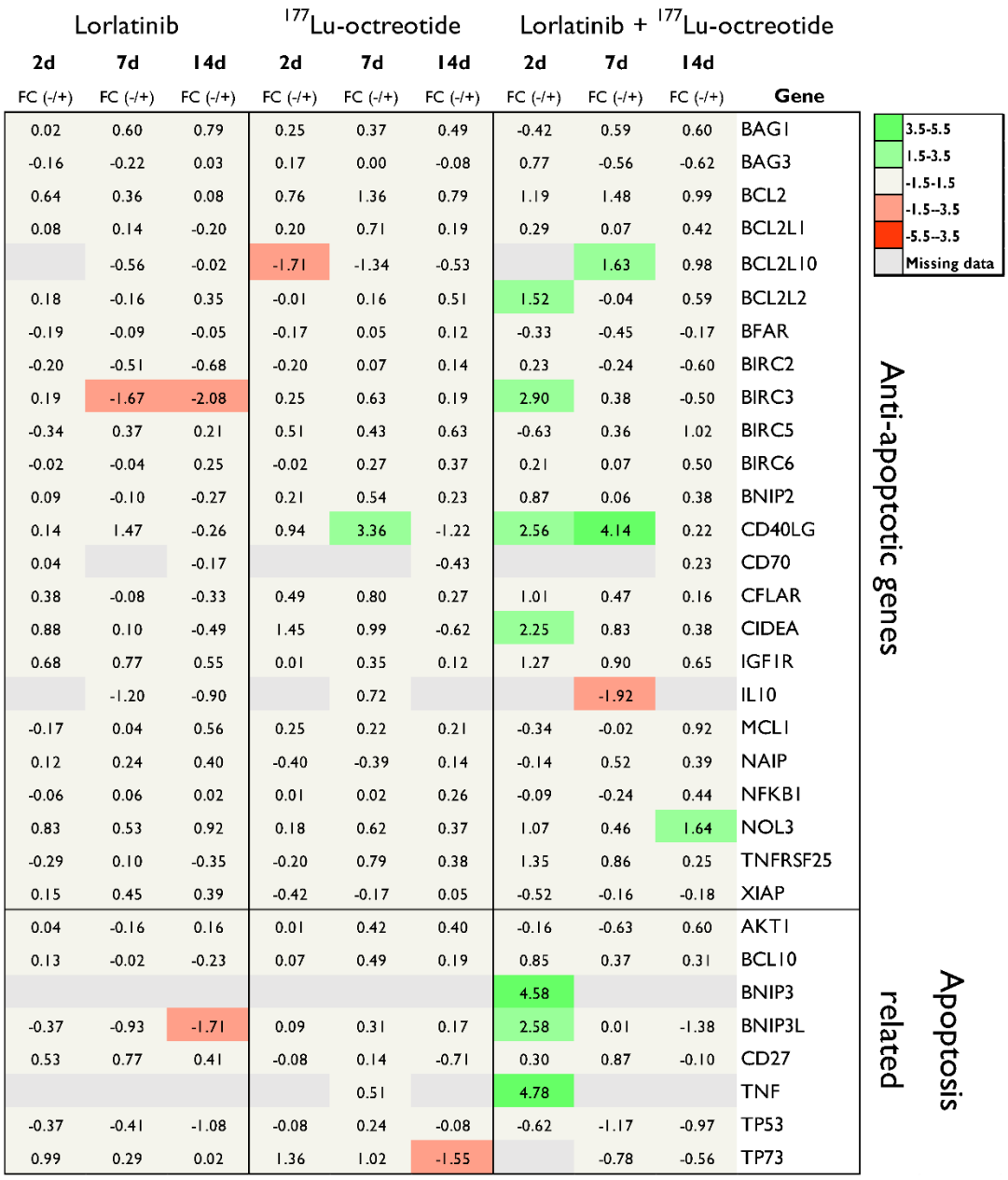

Figure 3. mRNA expression of 24 anti-apoptotic and 8 apoptosis related genes in tumor tissue (CLB-BAR) from mice treated with lorlatinib and/or ^{177}Lu-octreotide, expressed as fold change (FC) relative to controls. Tumors analysed were from mice sacrificed on day 2 (n=3), day 7 (n=3) or day 14 (n=4). Red and green colors represent down- and up-regulation, respectively, with $|FC| > 1.5$. Missing data are represented by gray color.

Treatment with ^{177}Lu-octreotide yielded expression changes in 9 unique genes of 79 detectable mRNAs (Figures 2-3). Six of the genes were classified as pro-apoptotic: *BCL2AI*, *CASPI*, *FASLG*, *TNFRSF10A*, *TNFRSF1B*, and *TNFSF8*. *BCL2AI*, *CASPI*, *FASLG*, and *TNFSF8* (day 14) were down-regulated, whereas *TNFRSF10A*, *TNFRSF1B*, and *TNFSF8* (day 7) were up-regulated (Figure 2). Two of the genes were classified as anti-apoptotic, *BCL2L10* and *CD40LG*, detected down- and up-regulated, respectively. *TP73*, classified as apoptosis-related, was found down-regulated.

Combination treatment with both lorlatinib and ^{177}Lu-octreotide resulted in differential expression of 23 unique genes of 78 detectable mRNAs (Figures 2-3). In total 13 pro-apoptotic genes: *BCL2LII*, *BID*, *CASP5*, *CASP8*, *CASP9*, *FAS*, *FASLG*, *GADD45A*, *HRK*, *LTA*, *LTBR*, *TNFRSF10A*, and *TNFRSF1B* exhibited differences in expression (Figure 2); only *BID* and *CASP8* were down-regulated,

 doi:10.20944/preprints202403.0251.v1

while the remaining genes were up-regulated. *CASP9* was up-regulated at both 2 and 7 days (Figure 2). Seven anti-apoptotic genes: *BCL2LI0*, *BCL2L2*, *BIRC3*, *CD40LG*, *CIDEA*, *IL10*, and *NOL3* were differentially expressed. Of these genes, *IL10* was the only down-regulated gene, the remaining genes were up-regulated (Figure 3). *CD40LG* was commonly found up-regulated after 2 and 7 days (Figure 3). Three apoptosis-related genes: *BNIP3*, *BNIP3L*, and *TNF* were down-regulated.

Figure 4 illustrates the transcriptional response for the statistically significant regulated genes ($|FC| > 1.5$, $p < 0.05$). The presented genes are relevant in both intrinsic (*BID*, *BNIP3L*, *CASP9*, and *HRK*) and extrinsic (*CASP8*, *CD40, FASLG, NOL3* and *TNFRSF10A*) apoptosis pathways. At 2 and 7 days after treatment start, the majority of significantly regulated genes were found in the combination group, and most of them were pro-apoptotic. Most of the genes were also upregulated compared with the control group. This pattern was not observed at 14 d.

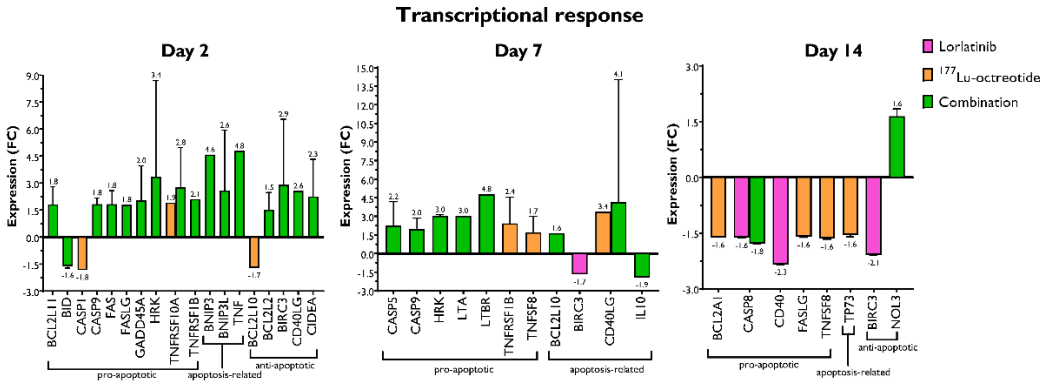

Figure 4. mRNA expression of pro-apoptotic, anti-apoptotic and apoptosis-related genes in human NB tumor tissue (CLB-BAR) from mice treated with lorlatinib and/or ^{177}Lu-octreotide, expressed as fold change (FC) relative to controls, on day 2 (n=3), day 7 (n=3) or day 14 (n=4). Only differentially regulated genes with $|FC| > 1.5$ are presented.

3.3. Immunohistochemical Analyses

We next analyzed apoptosis at the protein level in treated tumors employing antibodies against cleaved caspase 3 (CC3). Immunohistochemical examination identified CC3-positive cells (with nuclear staining) at days 2 and 14 after treatment start (Figure 5). Overall, we observed an increase in CC3-positive cells (Histoscore) in tumors from treated mice, with the exception of lorlatinib on day 2, with the highest Histoscore for combination-treated tumors on day 2. However, there was a large spread within the groups, and statistical significance was only observed at day 14 in the combination group.

 doi:10.20944/preprints202403.0251.v1

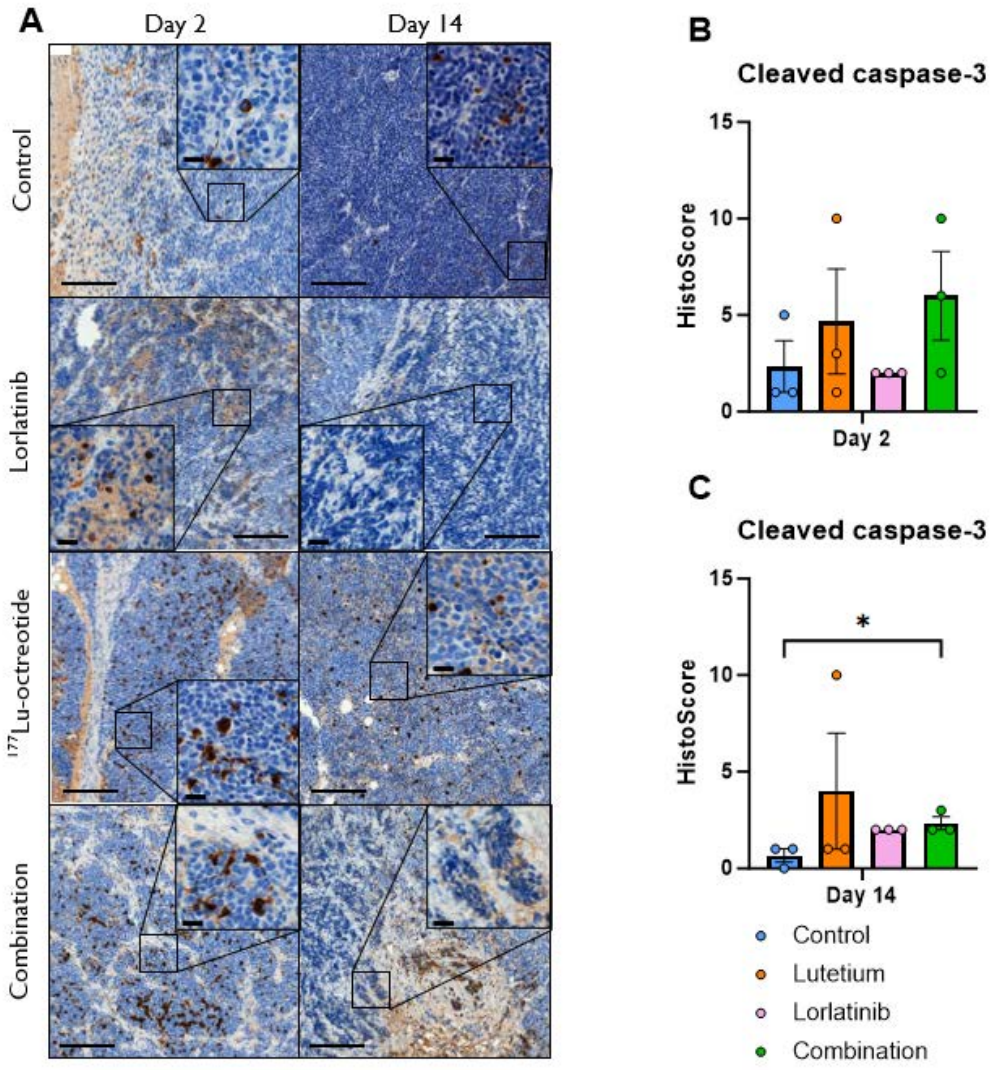

Figure 5. (**A**) Immunohistochemical staining for cleaved caspase-3 (CC3) in CLB-BAR tumors, 2 and 14 days post treatment. Lorlatinib was administered daily via gavage from day 0, ^{177}Lu-octreotide was administered i.v. on day 1 in both the combination group and the monotherapy and the control were i.v. injected with saline on day 1. Numerous CC3-positive cells were found in all images, with the highest intensity (visually) in the treated groups. Scale bars equals 200 µm and 20 µm (40× magnified inserts), respectively. (**B and C)** Distribution of CC3 Histoscore in CLB-BAR tumors at 2 (B) and 14 days (C) after treatment start for controls (blue), ^{177}Lu-octreotide (orange), lorlatinib (pink) and both ^{177}Lu-octreotide and lorlatinib in combination (green). The mean Histoscore value was calculated for each group based on the intensity (graded: 0, negative; 1, weak; 2, moderate; or 3, strong) and the percentage of positive cells. Error bars represent SEM. * represents $p<0.05$ calculated using Kruskal-Wallis test with Dunn's Multiple Comparison Test.

4. Discussion

Lorlatinib, a third-generation ALK inhibitor, has emerged as a treatment alternative for *ALK*-positive HR-NB [13]. Lorlatinib demonstrates enhanced activity and efficiency against *ALK*-mutations compared to previous generations of ALKi [10–12]. Nevertheless, several studies have reported lorlatinib-resistance in response to treatment, emphasizing the need for a multimodal therapy approach [15–18]. Systemic treatment with radiolabeled SSTAs, e.g. ^{177}Lu-octreotide, is successfully used for SSTR-overexpressing neuroendocrine tumors. To our knowledge, this is the first paper examining and reporting radiosensitization and synergistic antitumor effects in an *ALK*-amplified and SSTR-positive HR-NB xenograft model with lorlatinib and ^{177}Lu-octreotide.

 doi:10.20944/preprints202403.0251.v1

The present study was performed on CLB-BAR cells with *MYCN* amplification and *ALK* gain-of -function that may represent high-risk neuroblastomas [31,35]. In the mice, the CLB-BAR tumor volume reduction was moderate after treatment with ^{177}Lu-octreotide, which is consistent with results from a previous study in the same animal model, comparing effects of ^{177}Lu-octreotide and ^{177}Lu-octreotate [36]. Although biodistribution and biokinetics were most favorable for ^{177}Lu-octreotate, resulting in higher absorbed dose to tumor for ^{177}Lu-octreotate, the tumor volume reduction was somewhat better for ^{177}Lu-octreotide. It should be noted that the amount of ^{177}Lu-labeled SSTAs in these studies were on purpose low to enable visualization of additive or synergistic effects. These moderate therapeutic effects despite high uptake and retention in NB compared with other neuroendocrine tumors in similar models are unexpected, since the therapeutic effects in such studies were much more dramatic, with possibility to eradicate the tumor totally [37–40]. CLB-BAR has a high proliferation rate and tumor growth curve compared with other neuroendocrine tumor models of, e.g., intestinal origin, which might influence the therapeutic response [39]. Monotherapy with lorlatinib resulted in a cytostatic response. Thus, the present results are difficult to interpret, and may be related to certain properties in NB. Detailed signaling pathway analyses will be needed in order to understand the radioresistance in NB, and contribute to a better understanding, needed for future optimization of therapy with radiolabeled SSTAs. It is, however, clear that inhibition of ALK with lorlatinib may act to overcome some of the radioresistance in CLB-BAR NB cell xenografts.

ALK signals via several downstream pathways, having a considerable role in e.g. cell cycle progression, survival, DNA repair, proliferation, and angiogenesis, via Ras-extracellular signal-regulated kinase (Erk), PI3K-AKT-mTOR and Janus protein tyrosine kinase (JAK)-STAT [41–43]. However, how these signaling pathways are affected by irradiation, either alone or in combination with an ALKi, has not been explored. The present study demonstrated that treatment of CLB-BAR tumors with lorlatinib in combination with ^{177}Lu-octreotide synergistically reduced tumor volume and resulted in elevated transcription of genes involved in apoptosis. Several studies suggest that inhibiting critical mediators of the DNA damage response (DDR) can enhance radiosensitivity [42,44–47]. Dolman et al. demonstrated radiosensitization of NB cells by inhibiting the DNA-dependent protein kinase catalytic subunit (DNA-PKcs), playing a central role in the repair of DNA double-strand breaks (DSBs) via non-homologous end-joining (NHEJ) [44]. Further, combination of ^{177}Lu-octreotate and a p53 stabilizing drug showed better therapeutic effects compared to momnotherapy in NB cell spheroids and NB xenografts on mice [48,49]. Altogether, these findings indicate a possible role for DNA repair inhibition in the enhanced response to ^{177}Lu-octreotide combined with lorlatinib. Previous studies have illustrated the radiosensitizing effects of crizotinib, the first generation of ALKi, in combination with external radiation in ALK-positive non-small cell lung cancer (NSCLC) models [50,51]. The Akt kinase is one common mediator in both DDR and ALK pathways [52,53]. DNA damage sensors, e.g. DNA-PKcs, phosphorylate Akt in the DDR pathway due to, e.g. radiation induced DSBs [52]. Subsequently, phosphorylated Akt promotes NHEJ-mediated DSB repair and cell survival [52]. Hence, elevated levels of phosphorylated Akt is associated with malignant tumors and poor prognosis ([54,55]. Lorlatinib can, like crizotinib, aggravate NHEJ-mediated DSB repair by partially inhibiting Akt, a downstream signaling effector of ALK, and act as a radiosensitizer. However, a driving force in lorlatinib-resistance for HR-NB is activation of bypass pathways, such as EGFR, ErbB4, and RAS [15,56]. Other reported mechanisms causing ALKi-resistance are structural alterations in the kinase domain, leading to decreased binding of ALKi, as well as amplification of *ALK* [57]. Identifying the specific mechanisms underlying the drug-resistant properties that arise in response to ALKi treatments is essential for further treatment. In several patient case reports where relapse has occurred, multiple biopsies distributed throughout the treatment have been employed to modify the choice of ALKi to provide an optimal treatment strategy [58–61]. Of special interest is a case where an ALK-positive NSCLC gained resensitization to crizotinib after acquiring resistance to lorlatinib, highlighting the critical information provided via biopsies and the remarkable mechanisms behind ALKi-resistance [62].

Given the well-documented heterogeneous properties of NB [63] it may be necessary to eradicate tumor cells via various targets, aiming to eradicate multiple sub-populations of tumor cells and thus

 doi:10.20944/preprints202403.0251.v1

eliminate resistance. Based on our results, radiolabeled SSTAs may be a beneficial adjunctive treatment for disseminated SSTR-positive HR-NBs. Pilot trials with ^{177}Lu-octreotate, an alternative SSTA, have shown varied results for NB patients, highlighting the need for optimization according to each patient's specific tumor characteristics [27–29]. In addition, to avoid under-treatment, the biokinetics of the radiopharmaceutical need to be investigated before the start of the treatment. In the ongoing phase II trial with HR-NB patients, LuDO-N, ^{68}Ga-octreotide PET/CT examination will be used to determine activity levels of the two ^{177}Lu-octreotate administrations, not exceeding mean absorbed dose levels to the organs at risk (23 and 2.4 Gy to kidneys and whole body, respectively) [30]. Combining this information with information regarding eventual gain-of-function *ALK* mutations to, if possible, determine an appropriate ALKi for combination therapy is a further step to individualize the treatment.

The transcriptional response of the 84 genes involved in apoptosis provided another demonstration of the synergistic antitumor effect provided by the combination therapy. In total, 40 genes were up- or down-regulated, with the strongest differential gene expression observed in the ^{177}Lu-octreotide/lorlatinib combination therapy arm in which 26 genes were modulated, compared with 10 in response to ^{177}Lu-octreotide treatment, and only 4 with lorlatinib. Overall, a higher number of pro-apoptotic genes were up-regulated in the combination therapy at earlier time points, although more anti-apoptotic genes were also up-regulated at the same time. After statistical analysis of the ΔCt values (treated *vs.* control), only the combination treatment yielded a significant effect on the transcriptional response of genes within the Bcl-2 family (Table 1). Proteins of the Bcl-2 family are essential for apoptotic cell death in health and disease through different mechanisms [64–67]. Functionally categorized as pro-apoptotic or anti-apoptotic proteins within the Bcl-2 family, the imbalance of concentrations leads to cell survival or death [64,65]. Conversely, the tumor cells can continue their growth and progress if apoptosis can be inhibited, meaning that increased levels of anti-apoptotic proteins are associated with oncogenesis [65]. Our data demonstrated down-regulation of *BID* (BH3-interacting domain death agonist) on day 2, and up-regulation of *HRK* **(Harakiri, BCL2 interacting protein)** on day 7, both classified as pro-apoptotic genes. *BID* encodes for a protein (Bid) that connects the extrinsic apoptotic pathway with the intrinsic [68]. Cleaved Bid is translocated to the mitochondria and induces cytochrome c release, subsequently promoting downstream caspase activation [68]. Hrk is a BH3-only protein, encoded by *HRK*, and regulates apoptosis by displacing Bim or Bid from anti-apoptotic Bcl-xL, also leading to cytochrome c release and caspase activation [65,69].

Table 1. Functional characterization of differentially regulated genes after treatment with either lorlatinib, ^{177}Lu-octreotide, or both in combination. Differential gene expression is expressed as fold change (FC) relative to control. Only genes exhibiting $|FC| > 1.5$ and $p<0.05$ are presented. Lilac, yellow, and brown represent classification as pro-apoptotic, apoptosis-related, and anti-apoptotic genes, respectively.

Gene	Description	Protein family	FC	*p*	Time after treatment
CASP8	Caspase 8, apoptosis-related cysteine peptidase	Caspase family	-1.62	0.0003	14 days, Lorlatinib
CD40	CD40 molecule, TNF receptor superfamily member 5	TNF-receptor superfamily	-2.34	0.0001	14 days, Lorlatinib
BNIP3L	BCL2/adenovirus interacting protein 3-like	Pro-apoptotic subfamily within the Bcl-2 family	-1.71	0.0001	14 days, Lorlatinib
BIRC3	Baculoviral IAP repeat containing 3	Inhibition of apoptosis (IAP) family	-1.67 -2.08	0.0218 0.0005	7 days, Lorlatinib 14 days, Lorlatinib
FASLG	Fas ligand (TNF superfamily, member 6)	TNF superfamily	-1.60	0.0036	14 days, ^{177}Lu-octreotide

 doi:10.20944/preprints202403.0251.v1

TNFRSF10A	TNF receptor superfamily, member 10a	TNF-receptor superfamily	1.91	0.0004	2 days, ^{177}Lu-octreotide
TP73	Tumor protein p73	TP53 family	-1.55	0.0380	14 days, ^{177}Lu-octreotide
BID	BH3 interacting domain death agonist	Bcl–2 family	-1.62	0.0356	2 days, Combination
CASP8	Caspase 8, apoptosis-related cysteine peptidase	Caspase family	-1.78	0.0003	14 days, Combination
CASP9	Caspase 9, apoptosis-related cysteine peptidase	Caspase family	1.83 1.96	0.0011 0.0103	2 days, Combination 7 days, Combination
HRK	Harakiri, BCL2 interacting protein (contains only BH3 domain)	Bcl-2 family	3.02	0.0014	7 days, Combination
TNFRSF10A	TNF receptor superfamily, member 10a	TNF-receptor superfamily	2.75	0.0254	2 days, Combination
NOL3	Nucleolar protein 3 (apoptosis repressor with CARD domain)	Down-regulates activities of caspase 2, 8 and p53	1.64	0.0011	14 days, Combination

Other genes with their associated protein families belonged to caspase, tumor necrosis factor (TNF), and p53. The caspase family executes cell death via a cascade of activations. Various members are involved in both the extrinsic and intrinsic apoptotic pathways, and are classified as initiator or effector caspases [65,70]. *CASP8*, encoding the initiator caspase-8 (extrinsic pathway), was down-regulated on day 14 post-treatment with lorlatinib and the combination. Conversely, *CASP9*, encoding for the initiator caspase-9 (intrinsic pathway), was upregulated for the combination on days 2 and 7. TNF and TNF-receptor (TNFR) superfamilies are involved in the extrinsic signaling pathway of apoptosis and are activated by ligand binding to receptors [71]. Within the TNFR superfamily, *TNFRSF10A* was up-regulated on day 2 for both ^{177}Lu-octreotide and the combination. Whereas *CD40* was down-regulated at day 14 for lorlatinib. *FASLG*, encoding for Fas ligand belonging to the TNF superfamily, was down-regulated on day 14 for ^{177}Lu-octreotide. The tumor-suppressor family p53 is one of the most frequently mutated genes in cancer [72,73]; within this family, *TP73* was downregulated on day 14 for ^{177}Lu-octreotide. TP73 is involved in the regulation of, i.e., tissue development and inflammation [72,74].

Compared with two previous studies in a human small-intestine NET GOT1 mouse model where the transcriptional response was studied after treatment with ^{177}Lu-octreotate, some genes are commonly found. For example, *BNIP3L* (apoptosis-related) was up-regulated 41 days after administration with 15 MBq ^{177}Lu-octreotate. However, in the present study, *BNIP3L* was down-regulated after lorlatinib treatment on days 7 and 14 [75]. Besides comparing different tumor types, the relatively large time difference between the GOT1 and the present study may suggest that the tumors were in different phases after treatment, tumor regrowth vs. tumor shrinkage, and explain differences in the transcriptional response. In another study on the GOT1 model *BIRC3* (anti-apoptotic) was up-regulated one day post-administration with 30 MBq ^{177}Lu-octreotate [76], whereas it was down-regulated after lorlatinib treatment on days 7 and 14. A common up-regulation of the death receptor genes *TNFSRSF10A* and *TNFSRSF10B*, was also observed. *TNFSRSF10A* was up-regulated on day 2 after the combination treatment (present study), while *TNFSRSF10B* was up-regulated on days 1 and 7 post-treatment with 30 MBq ^{177}Lu-octreotate in the GOT1 study.

We complemented our gene expression analyses with immunohistochemistry for CC3 to study apoptosis at the protein level, as Caspase 3 has a central role in both apoptotic pathways as an executioner caspase. CC3 positivity was increased in response to treatment with the exception of lorlatinib on both day 2 and day 14, indicating an induction of apoptosis following treatment. However, the small sample size (n=3-4) and the large variability and non-normal distribution of the data resulted in only the combination treatment at 14 days having a statistically significant difference compared with control animals.

 doi:10.20944/preprints202403.0251.v1

In future studies, it would be interesting to combine fractionated/repeated administration of ^{177}Lu-octreotide in combination with lorlatinib. In a previous study in the same animal model, we observed that fractionated administration of ^{177}Lu-octreotate with short intervals resulted in a more prominent antitumor effect due to higher uptake in tumor cells because of recycling of SSTRs counteracting the likely SSTR saturation effects that prevail with single injection of higher amounts of SSTAs [36].

Treatment of HR-NB poses a challenge since most cases are diagnosed as an advanced, metastasized, and, therefore, inoperable disease. Although an intense treatment approach has been successful for certain patients, it is not always obvious which patients benefit most from them. And as the patient group is children, intensive treatments are avoided as much as possible because of the late effects. Hence, a multimodal approach could benefit two aspects: increased tumor control and mitigating side effects. Our study highlights the radiosensitizing nature of lorlatinib in NB-bearing mice. The fact that both treatments are systemic enables their combination in cases where the cancer have metastasized. Today, both lorlatinib and radiolabeled SSTAs are being studied separately in various phase I/II trials for HR-NBs, enabling the course for a possible combination for the cases where the prerequisites are met [14,30].

5. Conclusions

Synergistic antitumor effects were found when lorlatinib and ^{177}Lu-octreotide treatment was combined in an HR-NB xenograft mouse model. Combination therapy also had a more significant impact on expression of genes involved in apoptotic processes. The data suggest that inhibiting ALK signaling plays a role in the radiosensitization of radionuclide therapy with ^{177}Lu-octreotide, implying a potential for clinical application of combining ALKi with radiolabeled SSTAs for HR-NBs overexpressing SSTRs and ALK.

Author Contributions: AR: BH, RHP, JS, KH, and EFA designed and conceptualized the study. DEL and DP carried out the cell culturing. DP and AR conducted the animal experiments. HB and AR were responsible for the labeling of ^{177}Lu. AR, KS, and NR contributed to the RNA-extraction and the validation steps involved. KS and AR were responsible for the qPCR and the following data measurements. AR, EFA, NR, and JS contributed to the data analysis and interpretations. All authors reviewed and edited the manuscript. The authors read and approved the final manuscript. .

Funding: This study was supported by grants from the Swedish Research Council (EFA: 2021-02636; RHP: 2019-03914; BH: 2021-01192), the Swedish Cancer Society (EFA: CAN20/1293; RHP: CAN21/1459; BH: CAN21/1525), Swedish Childhood Cancer Foundation (EFA: PR2017-0057; RHP: PR2022-0029; BH: PR2021-0027), BioCARE - a National Strategic Research Program at University of Gothenburg, the Swedish state under the agreement between the Swedish government and the county councils – the ALF-agreement (ALFGBG-966074), the King Gustav V Jubilee Clinic Cancer Research Foundation, the Sahlgrenska University Hospital Research Funds, Wilhelm and Martina Lundgren Research Foundation, Assar Gabrielsson Cancer Research Foundation, Herbert & Karin Jacobsson Foundation, and Adlerbertska Research Foundation.

Institutional Review Board Statement: The study was conducted according to the guidelines of the Declaration of Helsinki, and approved by the Swedish Ethical Committee on Animal Experiments in Gothenburg (protocol code 2779-20 and date of approval 2020-08-26).".

Data Availability Statement: The original contributions presented in the study are included in the article/supplementary material, further inquiries can be directed to the corresponding author.

Conflicts of Interest: The authors declare no conflict of interest.

References

1. Umapathy: G.; Mendoza-Garcia, P.; Hallberg, B.; Palmer, R.H. Targeting anaplastic lymphoma kinase in neuroblastoma. *APMIS* **2019**, *127*, 288-302, doi:10.1111/apm.12940.
2. De Brouwer, S.; De Preter, K.; Kumps, C.; Zabrocki, P.; Porcu, M.; Westerhout, E.M.; Lakeman, A.; Vandesompele, J.; Hoebeeck, J.; Van Maerken, T.; et al. Meta-analysis of neuroblastomas reveals a skewed ALK mutation spectrum in tumors with MYCN amplification. *Clin Cancer Res* **2010**, *16*, 4353-4362, doi:10.1158/1078-0432.CCR-09-2660.

3. Eleveld, T.F.; Oldridge, D.A.; Bernard, V.; Koster, J.; Colmet Daage, L.; Diskin, S.J.; Schild, L.; Bentahar, N.B.; Bellini, A.; Chicard, M.; et al. Relapsed neuroblastomas show frequent RAS-MAPK pathway mutations. *Nat Genet* **2015**, *47*, 864-871, doi:10.1038/ng.3333.
4. Pugh, T.J.; Morozova, O.; Attiyeh, E.F.; Asgharzadeh, S.; Wei, J.S.; Auclair, D.; Carter, S.L.; Cibulskis, K.; Hanna, M.; Kiezun, A.; et al. The genetic landscape of high-risk neuroblastoma. *Nat Genet* **2013**, *45*, 279-284, doi:10.1038/ng.2529.
5. Berry, T.; Luther, W.; Bhatnagar, N.; Jamin, Y.; Poon, E.; Sanda, T.; Pei, D.; Sharma, B.; Vetharoy, W.R.; Hallsworth, A. The ALKF1174L mutation potentiates the oncogenic activity of MYCN in neuroblastoma. *Cancer cell* **2012**, *22*, 117-130.
6. Zhu, S.; Lee, J.-S.; Guo, F.; Shin, J.; Perez-Atayde, A.R.; Kutok, J.L.; Rodig, S.J.; Neuberg, D.S.; Helman, D.; Feng, H. Activated ALK collaborates with MYCN in neuroblastoma pathogenesis. *Cancer cell* **2012**, *21*, 362-373.
7. Schonherr, C.; Ruuth, K.; Kamaraj, S.; Wang, C.L.; Yang, H.L.; Combaret, V.; Djos, A.; Martinsson, T.; Christensen, J.G.; Palmer, R.H.; et al. Anaplastic Lymphoma Kinase (ALK) regulates initiation of transcription of MYCN in neuroblastoma cells. *Oncogene* **2012**, *31*, 5193-5200, doi:10.1038/onc.2012.12.
8. Morgenstern, D.A.; Bagatell, R.; Cohn, S.L.; Hogarty, M.D.; Maris, J.M.; Moreno, L.; Park, J.R.; Pearson, A.D.; Schleiermacher, G.; Valteau-Couanet, D.; et al. The challenge of defining "ultra-high-risk" neuroblastoma. *Pediatr Blood Cancer* **2019**, *66*, e27556, doi:10.1002/pbc.27556.
9. Johnson, T.W.; Richardson, P.F.; Bailey, S.; Brooun, A.; Burke, B.J.; Collins, M.R.; Cui, J.J.; Deal, J.G.; Deng, Y.-L.; Dinh, D. Discovery of (10 R)-7-Amino-12-fluoro-2, 10, 16-trimethyl-15-oxo-10, 15, 16, 17-tetrahydro-2H-8, 4-(metheno) pyrazolo [4, 3-h][2,5,11]-benzoxadiazacyclotetradecine-3-carbonitrile (PF-06463922), a macrocyclic inhibitor of anaplastic lymphoma kinase (ALK) and c-ros oncogene 1 (ROS1) with preclinical brain exposure and broad-spectrum potency against ALK-resistant mutations. *Journal of medicinal chemistry* **2014**, *57*, 4720-4744.
10. Syed, Y.Y. Lorlatinib: first global approval. *Drugs* **2019**, *79*, 93-98.
11. Zou, H.Y.; Friboulet, L.; Kodack, D.P.; Engstrom, L.D.; Li, Q.; West, M.; Tang, R.W.; Wang, H.; Tsaparikos, K.; Wang, J. PF-06463922, an ALK/ROS1 inhibitor, overcomes resistance to first and second generation ALK inhibitors in preclinical models. *Cancer cell* **2015**, *28*, 70-81.
12. Guan, J.; Tucker, E.R.; Wan, H.; Chand, D.; Danielson, L.S.; Ruuth, K.; El Wakil, A.; Witek, B.; Jamin, Y.; Umapathy, G.; et al. The ALK inhibitor PF-06463922 is effective as a single agent in neuroblastoma driven by expression of ALK and MYCN. *Disease Models & Mechanisms* **2016**, *9*, 941-952, doi:10.1242/dmm.024448.
13. Liu, T.; Merguerian, M.D.; Rowe, S.P.; Pratilas, C.A.; Chen, A.R.; Ladle, B.H. Exceptional response to the ALK and ROS1 inhibitor lorlatinib and subsequent mechanism of resistance in relapsed ALK F1174L-mutated neuroblastoma. *Molecular Case Studies* **2021**, *7*, a006064.
14. Goldsmith, K.C.; Park, J.R.; Kayser, K.; Malvar, J.; Chi, Y.Y.; Groshen, S.G.; Villablanca, J.G.; Krytska, K.; Lai, L.M.; Acharya, P.T.; et al. Lorlatinib with or without chemotherapy in ALK-driven refractory/relapsed neuroblastoma: phase 1 trial results. *Nat Med* **2023**, *29*, 1092-1102, doi:10.1038/s41591-023-02297-5.
15. Redaelli, S.; Ceccon, M.; Zappa, M.; Sharma, G.G.; Mastini, C.; Mauri, M.; Nigoghossian, M.; Massimino, L.; Cordani, N.; Farina, F.; et al. Lorlatinib Treatment Elicits Multiple On- and Off-Target Mechanisms of Resistance in ALK-Driven Cancer. *Cancer Research* **2018**, *78*, 6866-6880, doi:10.1158/0008-5472.Can-18-1867.
16. Mizuta, H.; Okada, K.; Araki, M.; Adachi, J.; Takemoto, A.; Kutkowska, J.; Maruyama, K.; Yanagitani, N.; Oh-Hara, T.; Watanabe, K. Gilteritinib overcomes lorlatinib resistance in ALK-rearranged cancer. *Nature communications* **2021**, *12*, 1-16.
17. Okada, K.; Araki, M.; Sakashita, T.; Ma, B.; Kanada, R.; Yanagitani, N.; Horiike, A.; Koike, S.; Oh-Hara, T.; Watanabe, K. Prediction of ALK mutations mediating ALK-TKIs resistance and drug re-purposing to overcome the resistance. *EBioMedicine* **2019**, *41*, 105-119.
18. Xie, B.; Qiu, Y.; Zhou, J.; Du, D.; Ma, H.; Ji, J.; Zhu, L.; Zhang, W. Establishment of an acquired lorlatinib-resistant cell line of non-small cell lung cancer and its mediated resistance mechanism. *Clinical and Translational Oncology* **2022**, *24*, 2231-2240.
19. Lamberts, S.W.J.; Krenning, E.P.; Reubi, J.-C. The Role of Somatostatin and Its Analogs in the Diagnosis and Treatment of Tumors. *Endocrine Reviews* **1991**, *12*, 450-482, doi:10.1210/edrv-12-4-450.
20. Baum, R.P.; Kluge, A.W.; Kulkarni, H.; Schorr-Neufing, U.; Niepsch, K.; Bitterlich, N.; van Echteld, C.J. [177Lu-DOTA] 0-D-Phe1-Tyr3-octreotide (177Lu-DOTATOC) for peptide receptor radiotherapy in patients with advanced neuroendocrine tumours: a phase-II study. *Theranostics* **2016**, *6*, 501.
21. Esser, J.-P.; Krenning, E.; Teunissen, J.; Kooij, P.; Van Gameren, A.; Bakker, W.; Kwekkeboom, D.J. Comparison of [177Lu-DOTA0, Tyr3] octreotate and [177Lu-DOTA0, Tyr3] octreotide: which peptide is preferable for PRRT? *European journal of nuclear medicine and molecular imaging* **2006**, *33*, 1346-1351.

22. Reubi, J.C.; Schär, J.-C.; Waser, B.; Wenger, S.; Heppeler, A.; Schmitt, J.S.; Mäcke, H.R. Affinity profiles for human somatostatin receptor subtypes SST1–SST5 of somatostatin radiotracers selected for scintigraphic and radiotherapeutic use. *European journal of nuclear medicine* **2000**, *27*, 273-282.
23. Uusijärvi, H.; Bernhardt, P.; Ericsson, T.; Forssell-Aronsson, E. Dosimetric characterization of radionuclides for systemic tumor therapy: influence of particle range, photon emission, and subcellular distribution. *Medical physics* **2006**, *33*, 3260-3269, doi:10.1118/1.2229428.
24. Uusijärvi, H.; Bernhardt, P.; Rösch, F.; Maecke, H.R.; Forssell-Aronsson, E. Electron- and positron-emitting radiolanthanides for therapy: aspects of dosimetry and production. *Journal of nuclear medicine : official publication, Society of Nuclear Medicine* **2006**, *47*, 807-814.
25. Swärd, C.; Bernhardt, P.; Ahlman, H.; Wängberg, B.; Forssell-Aronsson, E.; Larsson, M.; Svensson, J.; Rossi-Norrlund, R.; Kölby, L. [177Lu-DOTA0-Tyr3]-octreotate treatment in patients with disseminated gastroenteropancreatic neuroendocrine tumors: the value of measuring absorbed dose to the kidney. *World journal of surgery* **2010**, *34*, 1368-1372.
26. Romiani, A.; Spetz, J.; Shubbar, E.; Lind, D.E.; Hallberg, B.; Palmer, R.H.; Forssell-Aronsson, E. Neuroblastoma xenograft models demonstrate the therapeutic potential of 177Lu-octreotate. *BMC Cancer* **2021**, *21*, 950, doi:10.1186/s12885-021-08551-8.
27. Gains, J.E.; Bomanji, J.B.; Fersht, N.L.; Sullivan, T.; D'Souza, D.; Sullivan, K.P.; Aldridge, M.; Waddington, W.; Gaze, M.N. 177Lu-DOTATATE molecular radiotherapy for childhood neuroblastoma. *Journal of Nuclear Medicine* **2011**, *52*, 1041-1047.
28. Kong, G.; Hofman, M.S.; Murray, W.K.; Wilson, S.; Wood, P.; Downie, P.; Super, L.; Hogg, A.; Eu, P.; Hicks, R.J. Initial experience with gallium-68 DOTA-octreotate PET/CT and peptide receptor radionuclide therapy for pediatric patients with refractory metastatic neuroblastoma. *Journal of pediatric hematology/oncology* **2016**, *38*, 87-96.
29. Gains, J.E.; Moroz, V.; Aldridge, M.D.; Wan, S.; Wheatley, K.; Laidler, J.; Peet, C.; Bomanji, J.B.; Gaze, M.N. A phase IIa trial of molecular radiotherapy with 177-lutetium DOTATATE in children with primary refractory or relapsed high-risk neuroblastoma. *European Journal of Nuclear Medicine and Molecular Imaging* **2020**, *47*, 2348-2357.
30. Sundquist, F.; Georgantzi, K.; Jarvis, K.B.; Brok, J.; Koskenvuo, M.; Rascon, J.; van Noesel, M.; Grybäck, P.; Nilsson, J.; Braat, A. A Phase II Trial of a Personalized, Dose-Intense Administration Schedule of 177Lutetium-DOTATATE in Children With Primary Refractory or Relapsed High-Risk Neuroblastoma–LuDO-N. *Frontiers in pediatrics* **2022**, 167.
31. Fransson, S.; Hansson, M.; Ruuth, K.; Djos, A.; Berbegall, A.; Javanmardi, N.; Abrahamsson, J.; Palmer, R.H.; Noguera, R.; Hallberg, B.; et al. Intragenic anaplastic lymphoma kinase (ALK) rearrangements: translocations as a novel mechanism of ALK activation in neuroblastoma tumors. *Genes Chromosomes Cancer* **2015**, *54*, 99-109, doi:10.1002/gcc.22223.
32. Schmittgen, T.D.; Livak, K.J. Analyzing real-time PCR data by the comparative CT method. *Nature protocols* **2008**, *3*, 1101-1108.
33. Bliss, C.I. The toxicity of poisons applied jointly 1. *Annals of applied biology* **1939**, *26*, 585-615.
34. Sandblom, V.; Spetz, J.; Shubbar, E.; Montelius, M.; Ståhl, I.; Swanpalmer, J.; Nilsson, O.; Forssell-Aronsson, E. Gemcitabine potentiates the anti-tumour effect of radiation on medullary thyroid cancer. *Plos one* **2019**, *14*, e0225260.
35. Cazes, A.; Louis-Brennetot, C.; Mazot, P.; Dingli, F.; Lombard, B.; Boeva, V.; Daveau, R.; Cappo, J.; Combaret, V.; Schleiermacher, G.; et al. Characterization of Rearrangements Involving the ALK Gene Reveals a Novel Truncated Form Associated with Tumor Aggressiveness in Neuroblastoma. *Cancer Research* **2013**, *73*, 195-204, doi:10.1158/0008-5472.Can-12-1242.
36. Romiani. Comparison of ^{177}Lu-octreotate and ^{177}Lu-octreotide for treatment in human neuroblastoma-bearing mice (submitted).
37. Kölby, L.; Bernhardt, P.; Johanson, V.; Schmitt, A.; Ahlman, H.; Forssell-Aronsson, E.; Mäcke, H.; Nilsson, O. Successful receptor-mediated radiation therapy of xenografted human midgut carcinoid tumour. *British journal of cancer* **2005**, *93*, 1144-1151.
38. Swärd, C.; Bernhardt, P.; Johanson, V.; Schmitt, A.; Ahlman, H.; Stridsberg, M.; Forssell-Aronsson, E.; Nilsson, O.; Kölby, L. Comparison of [177Lu-DOTA0, Tyr3]-octreotate and [177Lu-DOTA0, Tyr3]-octreotide for receptor-mediated radiation therapy of the xenografted human midgut carcinoid tumor GOT1. *Cancer biotherapy & radiopharmaceuticals* **2008**, *23*, 114-120.
39. Elvborn, M.; Shubbar, E.; Forssell-Aronsson, E. Hyperfractionated Treatment with 177Lu-Octreotate Increases Tumor Response in Human Small-Intestine Neuroendocrine GOT1 Tumor Model. *Cancers* **2022**, *14*, 235.

40. Schmitt, A.; Bernhardt, P.; Nilsson, O.; Ahlman, H.; Kölby, L.; Forssell-Aronsson, E. Differences in biodistribution between 99mTc-depreotide, 111In-DTPA-octreotide, and 177Lu-DOTA-Tyr3-octreotate in a small cell lung cancer animal model. *Cancer biotherapy & radiopharmaceuticals* **2005**, *20*, 231-236.
41. Ducray, S.P.; Natarajan, K.; Garland, G.D.; Turner, S.D.; Egger, G. The transcriptional roles of ALK fusion proteins in tumorigenesis. *Cancers* **2019**, *11*, 1074.
42. Borenas, M.; Umapathy, G.; Lind, D.E.; Lai, W.Y.; Guan, J.; Johansson, J.; Jennische, E.; Schmidt, A.; Kurhe, Y.; Gabre, J.L.; et al. ALK signaling primes the DNA damage response sensitizing ALK-driven neuroblastoma to therapeutic ATR inhibition. *Proc Natl Acad Sci U S A* **2024**, *121*, e2315242121, doi:10.1073/pnas.2315242121.
43. Szydzik, J.; Lind, D.E.; Arefin, B.; Kurhe, Y.; Umapathy, G.; Siaw, J.T.; Claeys, A.; Gabre, J.L.; Van den Eynden, J.; Hallberg, B.; et al. ATR inhibition enables complete tumour regression in ALK-driven NB mouse models. *Nat Commun* **2021**, *12*, 6813, doi:10.1038/s41467-021-27057-2.
44. Dolman, M.E.M.; Van Der Ploeg, I.; Koster, J.; Bate-Eya, L.T.; Versteeg, R.; Caron, H.N.; Molenaar, J.J. DNA-dependent protein kinase as molecular target for radiosensitization of neuroblastoma cells. *PLoS One* **2015**, *10*, e0145744.
45. Toulany, M.; Kehlbach, R.; Florczak, U.; Sak, A.; Wang, S.; Chen, J.; Lobrich, M.; Rodemann, H.P. Targeting of AKT1 enhances radiation toxicity of human tumor cells by inhibiting DNA-PKcs-dependent DNA double-strand break repair. *Molecular cancer therapeutics* **2008**, *7*, 1772-1781.
46. Stronach, E.A.; Chen, M.; Maginn, E.N.; Agarwal, R.; Mills, G.B.; Wasan, H.; Gabra, H. DNA-PK mediates AKT activation and apoptosis inhibition in clinically acquired platinum resistance. *Neoplasia* **2011**, *13*, 1069-IN1035.
47. Dong, J.; Ren, Y.; Zhang, T.; Wang, Z.; Ling, C.C.; Li, G.C.; He, F.; Wang, C.; Wen, B. Inactivation of DNA-PK by knockdown DNA-PKcs or NU7441 impairs non-homologous end-joining of radiation-induced double strand break repair. *Oncology reports* **2018**, *39*, 912-920.
48. Lundsten, S.; Berglund, H.; Jha, P.; Krona, C.; Hariri, M.; Nelander, S.; Lane, D.P.; Nestor, M. p53-Mediated Radiosensitization of (177)Lu-DOTATATE in Neuroblastoma Tumor Spheroids. *Biomolecules* **2021**, *11*, doi:10.3390/biom11111695.
49. Berglund, H.; Salomonsson, S.L.; Mohajershojai, T.; Gago, F.J.F.; Lane, D.P.; Nestor, M. p53 stabilisation potentiates [(177)Lu]Lu-DOTATATE treatment in neuroblastoma xenografts. *Eur J Nucl Med Mol Imaging* **2024**, *51*, 768-778, doi:10.1007/s00259-023-06462-3.
50. Sun, Y.; Nowak, K.A.; Zaorsky, N.G.; Winchester, C.-L.; Dalal, K.; Giacalone, N.J.; Liu, N.; Werner-Wasik, M.; Wasik, M.A.; Dicker, A.P. ALK Inhibitor PF02341066 (Crizotinib) Increases Sensitivity to Radiation in Non–Small Cell Lung Cancer Expressing EML4-ALKPF02341066 Sensitizes EML4-ALK NSCLC Cells to Radiation Treatment. *Molecular cancer therapeutics* **2013**, *12*, 696-704.
51. Dai, Y.; Wei, Q.; Schwager, C.; Moustafa, M.; Zhou, C.; Lipson, K.E.; Weichert, W.; Debus, J.; Abdollahi, A. Synergistic effects of crizotinib and radiotherapy in experimental EML4–ALK fusion positive lung cancer. *Radiotherapy and Oncology* **2015**, *114*, 173-181.
52. Liu, Q.; Turner, K.M.; Alfred Yung, W.K.; Chen, K.; Zhang, W. Role of AKT signaling in DNA repair and clinical response to cancer therapy. *Neuro-Oncology* **2014**, *16*, 1313-1323, doi:10.1093/neuonc/nou058.
53. Iida, M.; Harari, P.M.; Wheeler, D.L.; Toulany, M. Targeting AKT/PKB to improve treatment outcomes for solid tumors. *Mutat Res* **2020**, *819-820*, 111690, doi:10.1016/j.mrfmmm.2020.111690.
54. Zheng, H.; Zhan, Y.; Zhang, Y.; Liu, S.; Lu, J.; Yang, Y.; Wen, Q.; Fan, S. Elevated expression of G3BP1 associates with YB1 and p-AKT and predicts poor prognosis in nonsmall cell lung cancer patients after surgical resection. *Cancer Medicine* **2019**, *8*, 6894-6903.
55. Opel, D.; Poremba, C.; Simon, T.; Debatin, K.-M.; Fulda, S. Activation of Akt predicts poor outcome in neuroblastoma. *Cancer research* **2007**, *67*, 735-745.
56. Berlak, M.; Tucker, E.; Dorel, M.; Winkler, A.; McGearey, A.; Rodriguez-Fos, E.; da Costa, B.M.; Barker, K.; Fyle, E.; Calton, E.; et al. Mutations in ALK signaling pathways conferring resistance to ALK inhibitor treatment lead to collateral vulnerabilities in neuroblastoma cells. *Molecular Cancer* **2022**, *21*, 126, doi:10.1186/s12943-022-01583-z.
57. Lin, J.J.; Riely, G.J.; Shaw, A.T. Targeting ALK: Precision Medicine Takes on Drug Resistance. *Cancer Discovery* **2017**, *7*, 137-155, doi:10.1158/2159-8290.Cd-16-1123.
58. Makuuchi, Y.; Hayashi, H.; Haratani, K.; Tanizaki, J.; Tanaka, K.; Takeda, M.; Sakai, K.; Shimizu, S.; Ito, A.; Nishio, K. A case of ALK-rearranged non–small cell lung cancer that responded to ceritinib after development of resistance to alectinib. *Oncotarget* **2018**, *9*, 23315.
59. Sharma, G.G.; Cortinovis, D.; Agustoni, F.; Arosio, G.; Villa, M.; Cordani, N.; Bidoli, P.; Bisson, W.H.; Pagni, F.; Piazza, R. A compound L1196M/G1202R ALK mutation in a patient with ALK-positive lung cancer with

acquired resistance to brigatinib also confers primary resistance to lorlatinib. *Journal of Thoracic Oncology* **2019**, *14*, e257-e259.
60. Takahashi, K.; Seto, Y.; Okada, K.; Uematsu, S.; Uchibori, K.; Tsukahara, M.; Oh-hara, T.; Fujita, N.; Yanagitani, N.; Nishio, M. Overcoming resistance by ALK compound mutation (I1171S+ G1269A) after sequential treatment of multiple ALK inhibitors in non-small cell lung cancer. *Thoracic Cancer* **2020**, *11*, 581-587.
61. Recondo, G.; Mezquita, L.; Facchinetti, F.; Planchard, D.; Gazzah, A.; Bigot, L.; Rizvi, A.Z.; Frias, R.L.; Thiery, J.P.; Scoazec, J.-Y. Diverse Resistance Mechanisms to the Third-Generation ALK Inhibitor Lorlatinib in ALK-Rearranged Lung CancerResistance to Lorlatinib in ALK-Rearranged Lung Cancer. *Clinical Cancer Research* **2020**, *26*, 242-255.
62. Shaw, A.T.; Friboulet, L.; Leshchiner, I.; Gainor, J.F.; Bergqvist, S.; Brooun, A.; Burke, B.J.; Deng, Y.-L.; Liu, W.; Dardaei, L. Resensitization to crizotinib by the lorlatinib ALK resistance mutation L1198F. *New England Journal of Medicine* **2016**, *374*, 54-61.
63. Gomez, R.L.; Ibragimova, S.; Ramachandran, R.; Philpott, A.; Ali, F.R. Tumoral heterogeneity in neuroblastoma. *Biochim Biophys Acta Rev Cancer* **2022**, *1877*, 188805, doi:10.1016/j.bbcan.2022.188805.
64. Youle, R.J.; Strasser, A. The BCL-2 protein family: opposing activities that mediate cell death. *Nature reviews Molecular cell biology* **2008**, *9*, 47-59.
65. Singh, R.; Letai, A.; Sarosiek, K. Regulation of apoptosis in health and disease: the balancing act of BCL-2 family proteins. *Nature reviews Molecular cell biology* **2019**, *20*, 175-193.
66. Spetz, J.K.E.; Florido, M.H.C.; Fraser, C.S.; Qin, X.; Choiniere, J.; Yu, S.J.; Singh, R.; Friesen, M.; Rubin, L.L.; Salem, J.E.; et al. Heightened apoptotic priming of vascular cells across tissues and life span predisposes them to cancer therapy-induced toxicities. *Sci Adv* **2022**, *8*, eabn6579, doi:10.1126/sciadv.abn6579.
67. Singh, R.; Yu, S.; Osman, M.; Inde, Z.; Fraser, C.; Cleveland, A.H.; Almanzar, N.; Lim, C.B.; Joshi, G.N.; Spetz, J.; et al. Radiotherapy-Induced Neurocognitive Impairment Is Driven by Heightened Apoptotic Priming in Early Life and Prevented by Blocking BAX. *Cancer Res* **2023**, *83*, 3442-3461, doi:10.1158/0008-5472.CAN-22-1337.
68. Yin, X.-m. Signal transduction mediated by Bid, a pro-death Bcl-2 family proteins, connects the death receptor and mitochondria apoptosis pathways. *Cell research* **2000**, *10*, 161-167.
69. Kaya-Aksoy, E.; Cingoz, A.; Senbabaoglu, F.; Seker, F.; Sur-Erdem, I.; Kayabolen, A.; Lokumcu, T.; Sahin, G.N.; Karahuseyinoglu, S.; Bagci-Onder, T. The pro-apoptotic Bcl-2 family member Harakiri (HRK) induces cell death in glioblastoma multiforme. *Cell death discovery* **2019**, *5*, 64.
70. Fan, T.-J.; Han, L.-H.; Cong, R.-S.; Liang, J. Caspase family proteases and apoptosis. *Acta biochimica et biophysica Sinica* **2005**, *37*, 719-727.
71. Dostert, C.; Grusdat, M.; Letellier, E.; Brenner, D. The TNF family of ligands and receptors: communication modules in the immune system and beyond. *Physiological reviews* **2019**, *99*, 115-160.
72. Morris, S.M. A role for p53 in the frequency and mechanism of mutation. *Mutation Research/Reviews in Mutation Research* **2002**, *511*, 45-62.
73. Marei, H.E.; Althani, A.; Afifi, N.; Hasan, A.; Caceci, T.; Pozzoli, G.; Morrione, A.; Giordano, A.; Cenciarelli, C. p53 signaling in cancer progression and therapy. *Cancer Cell Int* **2021**, *21*, 703, doi:10.1186/s12935-021-02396-8.
74. Zawacka-Pankau, J.E. The Role of p53 Family in Cancer. *Cancers (Basel)* **2022**, *14*, doi:10.3390/cancers14030823.
75. Spetz, J.; Rudqvist, N.; Langen, B.; Parris, T.Z.; Dalmo, J.; Schüler, E.; Wängberg, B.; Nilsson, O.; Helou, K.; Forssell-Aronsson, E. Time-dependent transcriptional response of GOT1 human small intestine neuroendocrine tumor after 177Lu [Lu]-octreotate therapy. *Nuclear Medicine and Biology* **2018**, *60*, 11-18.
76. Rassol, N.; Andersson, C.; Pettersson, D.; Al-Awar, A.; Shubbar, E.; Kovacs, A.; Akerstrom, B.; Gram, M.; Helou, K.; Forssell-Aronsson, E. Co-administration with A1M does not influence apoptotic response of (177)Lu-octreotate in GOT1 neuroendocrine tumors. *Sci Rep* **2023**, *13*, 6417, doi:10.1038/s41598-023-32091-9.